The ABB Power Transmission Test Case

Mats Larsson
Corporate Research
ABB Schweiz AG
mailto:Mats.Larsson@ch.abb.com

Feb 12, 2002
revised Oct 22, 2002

Contents

1 Introduction

This report describes a test case intended for test of control synthesis and analysis of hybrid systems. The test case illustrates voltage stability and the emergency control that may be necessary to avoid collapse and the subsequent blackout in the power system following severe disturbances.

Even though the power system considered here is trivially small (from the power engineer's point of view) it contains some interesting mechanisms that makes it suitable for this type of study. Firstly, there is hybrid behaviour that arises from discrete control logic in the generator and voltage controllers that are embedded in these components. Secondly, there is nonlinearity in the continuous time dynamics of the system.

The computer implementation of the test system is available as Modelica code as well as SIMULINK SimStruc.

In later version of the test case, also a power system of realistic size will be modelled, resulting in a control problem with around 50 control inputs, as many disturbance inputs and perhaps 100 controlled outputs.

Section 5 is a short tutorial to the control of voltage in power system and voltage stability in particular. It has been written to introduce readers not familiar with power system to the voltage control application.

Section 2 contains the description of the actual test case and the appendix contains detailed documentation of the Modelica test case, including each component's representation in the supplied models and reasonable operational limits on relevant process variables.

2 ABB Test Case

This note provides additional documentation about the ABB test case. The models have been implemented in Modelica (Tiller, 2001). See the source code and its HTML documentation for a detailed information about the implementation of the various component models.

The basic power system contains two generators and three lines as shown in Figure 1. Additionally there is a transformer that can regulate the (customer) voltage at Bus 4 and a capacitor bank that can support the voltage at Bus 3. The generator Ginf is a model of the surrounding network which is assumed to be strong, and generator G1 is equipped with a voltage regulator with a field voltage limit at 2.2 p.u. The transformer T1 is equipped with a voltage regulator modelled by a state-machine. These controllers constitute a *primary* control layer which should preferably be not be modified. The task of the the test case is to design a secondary control layer which has access to the following input signals:

- CapStep–an integer variable that can take the values [0,1,2,3]. Each step corresponds to 0.1 p.u. of reactive compensation. Increase of this control will increase the voltage at Bus 3, however the effectiveness of the control is highly dependent on the operating point.
- LoadStep–an integer variable that can take the values [0,1,2,3]. Each step corresponds to disconnection of 5 % of the load at Bus 4. This action will always effectively increase the voltage at Bus 4. However, the use of load disconnection must be limited to extreme cases where it not possible to stabilize the voltage using a combination of the other two control.
- TapVref–a continuous variable that can take values in the interval [0.9..1.1] and corresponds to the setpoint of the voltage regulator of transformer T1 that regulates the voltage at Bus 4.

In addition there is a disturbance input (which can be assumed measured):

- Faulted–a boolean input indicating whether or not there has been a fault on line L3. The disconnection of the line is modelled by a change of its impedance from 0.5 to 1.5 p.u. and corresponds to the disconnected of two out of three parallel lines.

Three outputs have been assigned:

- V2–the voltage at bus 2, close to the generator voltage. This voltage is regulated by generator G1 so it it kept constant. However, when the generator becomes overloaded (that is, Efd≥Efmax) the generator loses its voltage control capability and the voltage V2 may drop.
- V3–the voltage at bus 3 can be controlled using the capacitor at Bus 3.

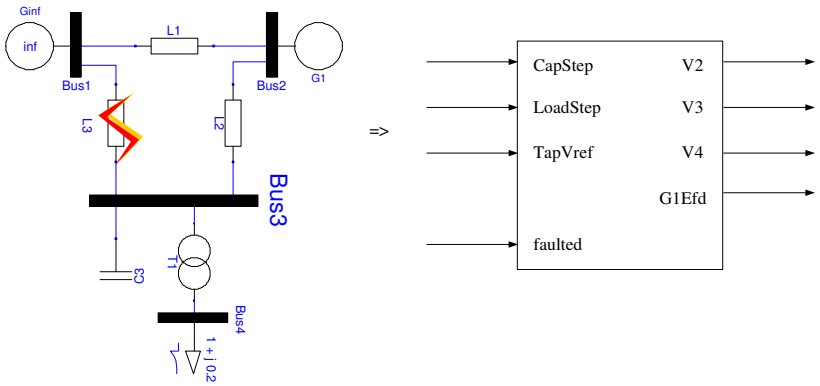

Figure 1: The physical power system and its hybrid system representation.

- V4–the voltage at Bus 4 can be controlled by the tap changer on the transformer T1. However, after the fault has been applied the system becomes heavily stressed and V3 decreases as V4 is increased. When there is no longer support of the voltage at bus 2 and 3 from the generator G1, this effect becomes dominant and each (upwards) tap step made on transformer actually decreases the voltage of Bus 4.

2.1 Control Objectives

The aim of the emergency control is to stabilize all voltages at values above 0.9 p.u following the fault. A secondary aim to to minimize the amount of load shedding applied. The tertiary objective is to keep the voltage at bus 4 close to 1 p.u, and to minimize the amount of capacitor control required to do so. That is, load shedding can be used to fulfil the primary objective but not the the tertiary.

Computational delay times of up to 30 s are acceptable, however all controls are more effective when applied as soon as possible following the fault.

2.2 Example Simulations

This sections presents some example simulations and demonstrates the application of emergency controls.

Figure 2 shows the system response to the fault applied at 100 s. The voltage drop following directly from the fault is not severe, however the load dynamics and tap changer control drives generator G1 towards its capability limit. When this is reached at 224 s, the generator voltage drops and the system collapse follows at about 390 s.

Figure 3 shows the response when the transformer voltage setpoint is reduced to 0.92 p.u. at time 110 s. The response is similar to that without emergency control, however the collapse occurs slightly later, at 410 s. Thus, we can

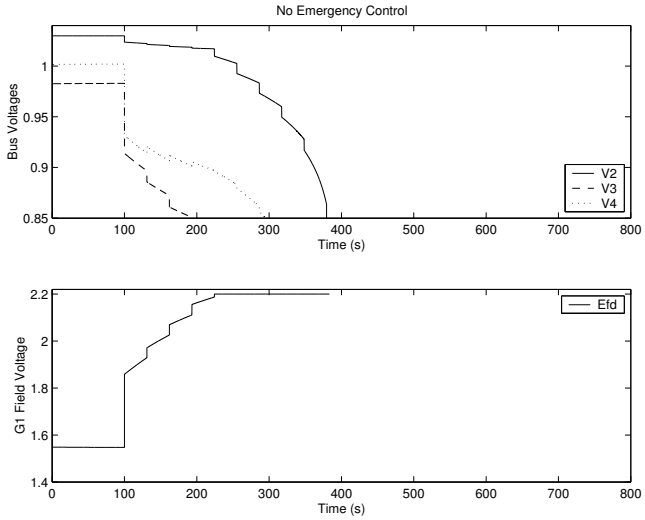

Figure 2: Response to the fault without emergency control.

conclude that the setpoint change alone is not sufficient to arrest the collapse, but it appears to have a positive influence since the collapse is delayed.

Figure 3 shows the response when additional reactive support is provided by stepping up the capacitor bank C1 at 110 s. This relieves generator G1 of some reactive load and it is kept slightly below its field voltage limit. Therefore, the voltages eventually stabilize but the voltage of Bus 3 is still unacceptably low.

Figure 5 shows the response when load is shed at time 110 s. This relieves generator G1 of both active and reactive load and it is kept well below its field voltage limit and the scenario is therefore stable. Also, the voltage drop over the remaining lines is reduced and also the voltage of Bus 3 is acceptable.

Figure 6 shows the response when a combination of additional capacitor and tap setpoint change at time 110 s. The voltages are stabilized without load shedding at acceptable levels. According to the control objectives, these are the correct controls to apply.

2.3 Simulink Model Files

The following files related to the full version of the test case are distributed:

- `primarycontrolledd.dll` – the binary for the SimStruc model
- `abbvars.mat` – .mat file containing parameter data and other variables necessary for simulation
- `testsim.mdl` – Simulink shell model to simulate the test case
- `primarycontrolled.mdl` – Simulink model with external inputs/outputs that for example can be used to programmatically access the model

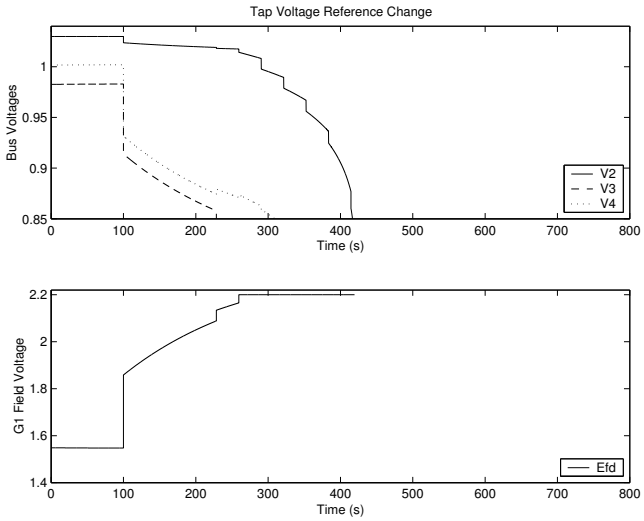

Figure 3: Response to the fault with adjustment of transformer voltage regulator setpoint.

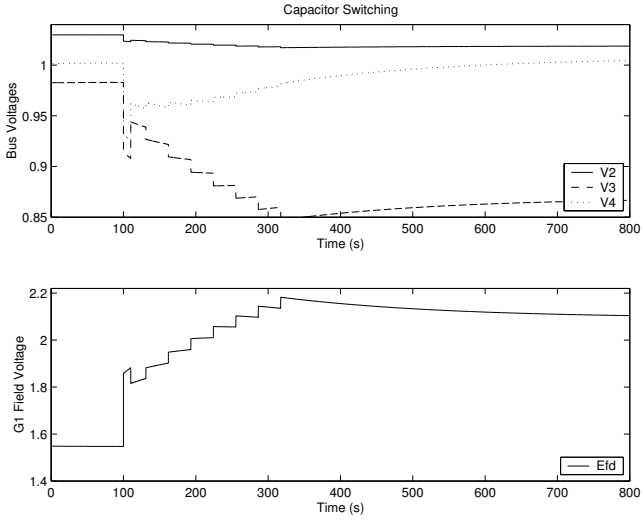

Figure 4: Response to the fault with connection of additional capacitor bank.

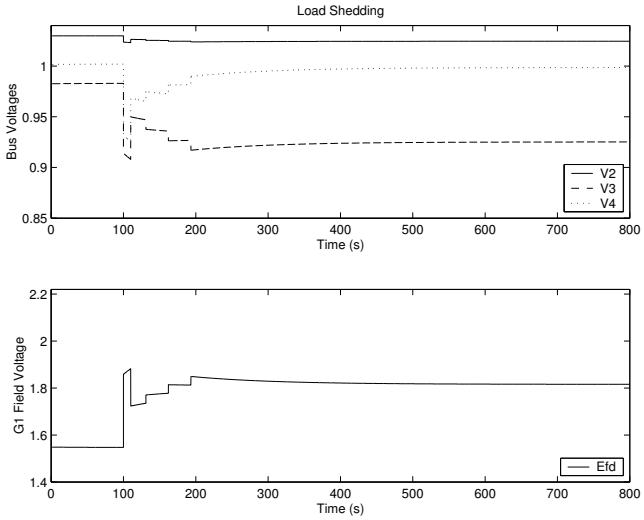

Figure 5: Response to the fault with load shedding.

- `scensim.m` – Example Matlab script that generates Figures 2–6.
- `test_mod.m` – Example Matlab script that shows how to properly initialize discrete and continuous state variables when the simulation is started programmatically.
- `test_mod_x0.mdl` Simulink shell model used by`test_mod.m`.
- `testsim2.mdl`,`scensim.m` – Simulink version of the test case split into continuous and discrete parts. Since Simulink has trouble handling algebraic loops, a number of spikes occur during simulation. The use of this model is not recommended, and was used only to verify that the individual continuous and discrete submodels are working correctly.

Note that since the Simulink interface of Dymola (Elmqvist et al., 2000), that has been used to produce the Modelica model, does not yet fully support state-event handling, the Simulink model must be simulated with state-event detection disabled as has been done in the files `testsim.mdl` and `openloop.mdl`. In this version, both continuous and discrete behavior have been aggregated in the same model.

Note that the discrete states in the model are initialized with the values given in the parameter vectors when a Simulink simulation is started. To define the initial values of the continuous and discrete states at the start of a simulation, the correct updates must be made in the parameter vector `primarycontrolled.p`. This version of the testcase also provides many auxilliary variables that can be used for debug purposes.

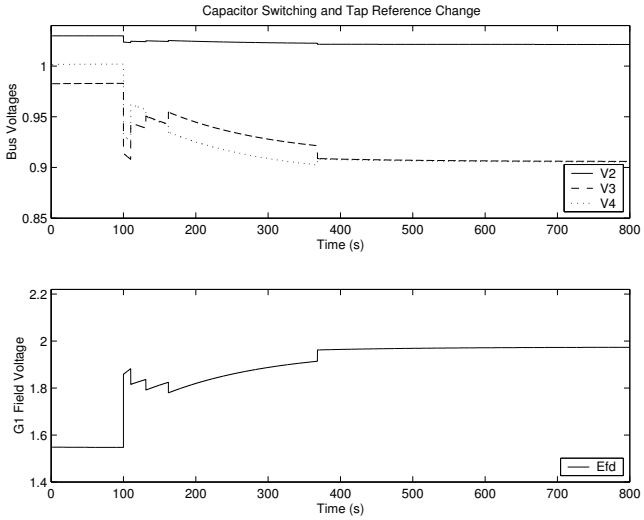

Figure 6: Response to the fault with a combination of additional capacitor bank and adjustment of transformer voltage regulator setpoint.

3 Decomposition of Models into Continuous and Discrete Parts

As shown in Figure 7, the hybrid system in Figure 1 can be decomposed into one non-linear continuous part (without any hybrid dynamics) and one hybrid part. The continuous part essentially corresponds to an uncontrolled (open-loop) model of the power system and the hybrid part to the primary control systems that are applied.

3.1 Model of Continuous Open-loop Part

3.1.1 Simulink Model Files

The open loop power system can be represented on the form

$$\dot{x} = f(x, u) \tag{1}$$

$$y = g(x, u) \tag{2}$$

where $x = [Load.xp, Load.xq]$ is the continuous state vector, $y = [V2, V3, V4]$ is the output vector and
$u = [CapStep, LoadStep, TrStep, G1Efd, faulted]$ is the input vector.

Once it has been initialized by a call to the MATLAB m-file `cont_init.m`, the openloop part can be programmatically accessed through the m-files `cont_f.m` and `cont_g.m`. The Matlab script `testopenloop.m` which generators Figure 8 shows how to call these functions. These functions also needs the SIMULINK

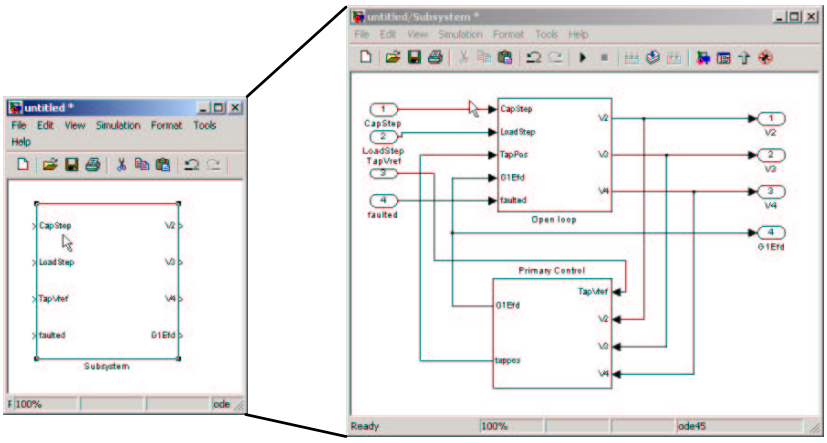

Figure 7: Decomposition of the hybrid system into its' continuous and discrete parts.

models openloop.mdl and openloop2.mdl which acts as wrappers for the mex S-functions that have been generated from the Modelica model. Additionally to the signals in y, also the state vector x has been included as ouputs of the mex S-function.

Figure 8 illustrates the nonlinearity in the continuous which is only slight, and occurs only at very low voltages.

3.2 Model of Discrete Part

The hybrid part essentially consists of a state machine that controls the position of the tap changer at transformer T1 from a voltage measurements on the secondary side of the transformer, and a proportional controller with a limiter, that controls the field voltage of generator G1. The best documentation of the discrete part is so far the Modelica code itself.

3.3 Future Work

In a later version, also a power system of realistic size will be modelled. Optimal control of such a system has previously studied by e.g. Larsson (2000a).

4 Acknowledgement

Most of the new developments since the original version have been suggested by Tobias Geyer at ETH Zürich. Thanks to him the test case is now slightly closer to the form a real control engineer wants it.

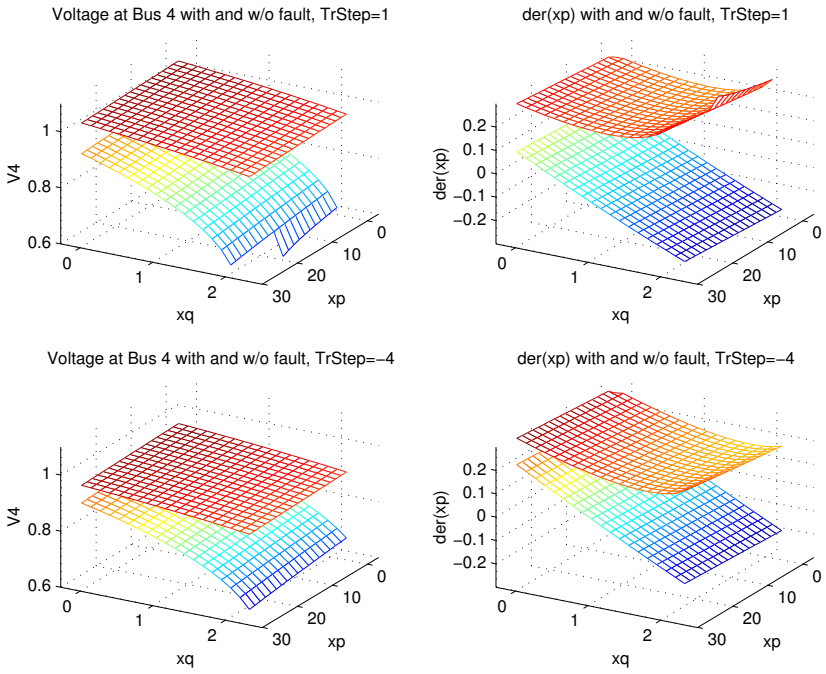

Figure 8: Illustration of nonlinearity in the continuous dynamics.

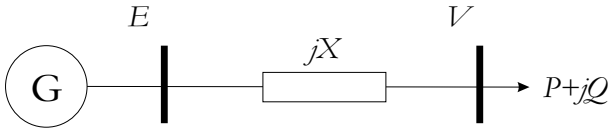

Figure 9: Single line diagram of a simple radial power system.

5 Voltage Stability Tutorial

This section outlines some of the fundamentals of voltage control and stability and highlights some of the more important aspect and has been adapted from Larsson (2000a). Readers requiring more detailed descriptions are recommended to consult the textbooks by Taylor (1994) and Van Cutsem and Vournas (1998). It is assumed that the reader is already familiar with basic circuit theory and the associated phasor computations.

5.1 Transfer of Active and Reactive Power

Consider the circuit in Figure 9. A strong source with voltage E supplies a remote load through a transmission line modelled as a series reactance. The receiving end voltage V and angle δ depend on the active and reactive power transmitted through the line. The active and reactive power received at the load end can be written (Van Cutsem and Vournas, 1998)

$$P = -\frac{EV}{X}\sin\delta \tag{3}$$

$$Q = \frac{EV}{X}\cos\delta - \frac{V^2}{X} \tag{4}$$

After eliminating δ using the trigonometric identity we get

$$\left(Q + \frac{V^2}{X}\right)^2 + P^2 = \left(\frac{EV}{X}\right)^2 \tag{5}$$

Solving for V^2 yields

$$V^2 = \frac{E^2}{2} - QX \pm X\sqrt{\frac{E^4}{4X^2} - P^2 - Q\frac{E^2}{X}} \tag{6}$$

Thus, the problem has real positive solutions if

$$P^2 + Q\frac{E^2}{X} \leq \frac{E^4}{4X^2} \tag{7}$$

This inequality shows which combinations of active and reactive power that the line can supply to the load. Substituting the short-circuit power at the receiving end, $S_{sc} = E^2/X$, we get

$$P^2 + QS_{sc} \leq \left(\frac{S_{sc}}{2}\right)^2 \tag{8}$$

Some preliminary observations that can be made from the condition (8) are:

- The maximum possible active power transport is $S_{sc}/2$ for $Q = 0$.
- The maximum possible reactive power transport is $S_{sc}/4$ for $P = 0$.
- An injection of reactive power at the load end, i.e., $Q < 0$ increases the transfer limit for active power.
- The transfer limits are proportional to the line admittance and to the square of the feeding voltage E.

Thus, it appears more difficult to transfer reactive than active power over the inductive line, and it seems that reactive power transfer can influence the ability of the line to carry active load. Furthermore, assume for now that the load has admittance characteristics, that is, the active and reactive power received by the load can be written

$$P + jQ = V^2\, G(1 + j\tan(\phi)) \tag{9}$$

Thus, the load produces reactive power for leading power factor ($\tan(\phi) < 0$) and absorbs reactive power for lagging power ($\tan(\phi) > 0$). After normalizing equations (6) and (9) using

$$p = P/S_{sc}, \qquad q = Q/S_{sc} \tag{10}$$

$$v = V/E, \quad g = G/(1/X)) \tag{11}$$

Using normalized quantities, the positive solution to (6) can be written

$$v = \frac{1}{\sqrt{g^2 + (1 + g\tan(\phi))^2}} \tag{12}$$

Not surprisingly, there is no voltage drop over the line when the load admittance is zero and the load voltage approaches zero as the load admittance increases towards infinity. Figure 10 shows the so-called onion surface (Van Cutsem and Vournas, 1998) given by (12) drawn in the pqv-space. It illustrates the relationship between receiving end voltage and transferred active and reactive power, and each point on the surface corresponds to a feasible operating point. The surface visualizes the set of operating points that the combined generation and transmission system can sustain. The actual operating point is determined by the apparent load admittance, and the stability of this operating point is determined jointly by the slope of the surface and the load characteristics. The stability of operating points will be dealt with in Section 5.5. The solid lines drawn on the surface correspond to operating points with varying g and constant $\tan(\phi)$ (shown by the number beside each line). The dashed line around the "equator" of the surface corresponds to the transfer limit according to the condition (8).

Figure 11 shows so-called pv-curves (Taylor, 1994), which are projections of the solid lines drawn on the onion surface onto the pv-plane. The rightmost

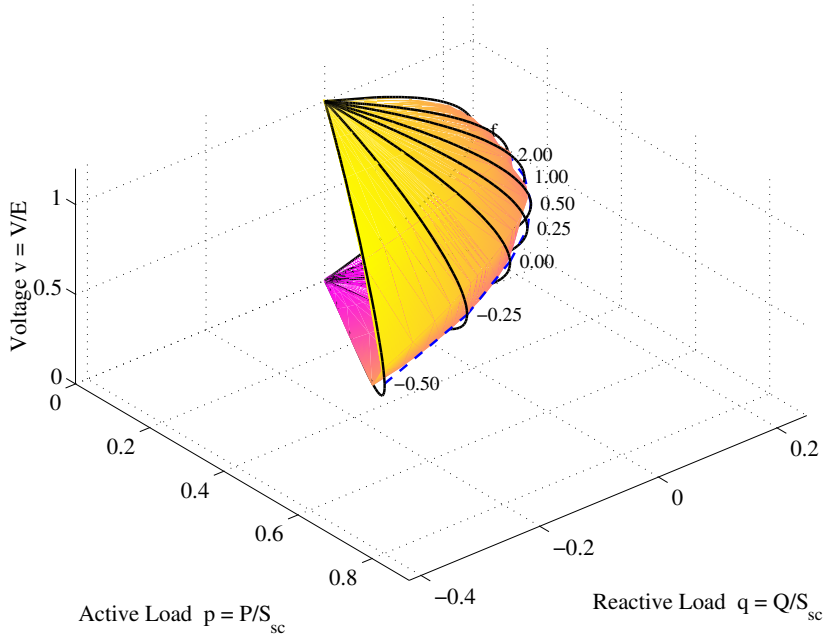

Figure 10: The so-called onion surface (Van Cutsem and Vournas, 1998) as given by Equation (12) drawn using normalized load quantities.

point of each *pv*-curve marks the maximum active power transfer for a particular power factor. The corresponding voltage shown by the dashed curve is therefore often referred to as the *critical* voltage and the active loading as the *theoretical transfer limit*. The critical voltage and theoretical transfer limit increase with decreasing $\tan(\phi)$. As will later be demonstrated in Section 5.5, only operating points on the upper half of the *pv*-curve are stable when the load has constant power characteristics.

According to the condition (8), the maximum power a purely active load can theoretically receive through the line is half the short-circuit power at the load bus, given that no reactive power is received at the load end. The shaded region indicates normal operation of a line–the voltage of both ends of the line is normally kept close to the rated voltage of the line. Typical limits are ± 5 % deviation from nominal voltage or up to ± 5 % in emergency cases. The receiving end voltage at the theoretical transfer limit with a purely active load is $1/\sqrt{(2)} \approx 0.71$, which is normally considered unacceptable. The *practical transfer limit* is therefore about 35 % of the short-circuit power or even lower when the load has a lagging power factor[1]. Capacitor banks connected at the load end are often used to increase the load end voltage and thereby the practical transfer limit. Reactive power is then being produced locally instead of transferred by the line,

[1]The limit referred to here is the voltage-drop limit.

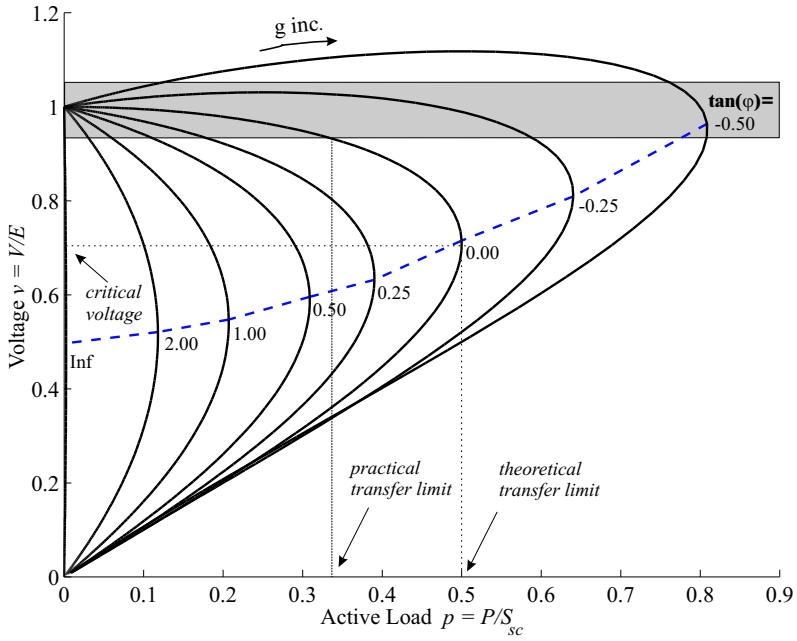

Figure 11: The onion surface projected onto the *pv*-plane. The practical and theoretical transfer limits and the critical voltage is given for $tan(\phi) = 0$. The shaded region indicates normal operation of the line.

and the apparent power factor of the load (as seen from the transmission system) is enhanced. The operating point then shifts to another *pv*-curve corresponding to a lower value of $\tan(\phi)$. When the operating point is on the upper part of the *pv*-curve, which is the case under normal operation, this corresponds to higher voltage.

The *pv*-curves also indicate the *stiffness* of system with respect to active power load variations. By overcompensating the load, such that the apparent $\tan(\phi)$ becomes negative, transfer beyond half the short-circuit power with voltage close to nominal levels can theoretically be accommodated. Note however that the sensitivity to load variations, which corresponds to the steepness of the *pv*-curve within the shaded region, is much larger in an overcompensated system. Another important aspect is that the critical voltage is brought closer to nominal voltage. It will be shown in Section 5.5 that for constant power load characteristics, the theoretical transfer limit coincides with the voltage stability limit. Thus, the difference between the critical voltage and the voltage of the current operating point can be used as a robustness measure in terms of voltage. Similarly, the difference between the current loading and the theoretical transfer limit can be used as a robustness measure in terms of active power.

5.2 Sources and Sinks of Reactive Power

The previous section showed that the voltage at the receiving end is highly dependent on the absorption or injection of reactive power by the load. The control of voltage is in fact closely related to the control of reactive power. An injection of reactive power at a bus that is not directly voltage regulated by a generator will in general increase the voltage of that bus and its surrounding network.

The most important sources and sinks of reactive power in power systems are listed below.

- Overhead (AC) lines generate reactive power under light load since their production due to the line shunt capacitance exceeds the reactive losses in the line due to the line impedance. Under heavy load, lines absorb more reactive power than they produce.
- Underground (AC) cables always produce reactive power since the reactive losses never exceed the production because of their high shunt capacitance.
- Transformers always absorb reactive power because of their reactive losses. In addition, transformers with adjustable ratio can shift reactive power between their primary and secondary sides.
- Shunt capacitors generate reactive power.
- Shunt reactors absorb reactive power.
- Loads seen from the transmission system are usually inductive and therefore absorb reactive power.
- Synchronous generators, synchronous condensers and static VAr compensators can be controlled to regulate the voltage of a bus and then generate or absorb reactive power depending on the need of the surrounding network.
- Series capacitors are connected in series with highly loaded lines and thereby reduce their reactive losses.

Controllable components are generally classified as either *static* or *dynamic*. Static components such as shunt capacitors and reactors can be regulated in fixed discrete steps and with some time delay. They can therefore not be used to improve system response to short-term phenomena such as those related to the generator mechanical or flux dynamics. Hunting phenomena involving such discrete compensation devices may occur in heavily compensated systems (Yorino et al., 1997; Larsson et al., 1998), which have poor voltage stiffness properties. They are however very reliable and cost-effective for reactive compensation in the long term as long as they are used in moderate amounts. On the other hand, dynamic compensation devices, such as synchronous condensers and generators, and static var compensators, can be controlled rapidly and continuously. Thanks to their short response time, they can be used to improve

short-term as well as long-term response of the power system. The drawback is that dynamic compensation is 5-10 times more expensive per Mvar of compensation (Taylor, 2000). Some loads, for example arc furnaces, create fast voltage fluctuations with frequencies of about 2-10 Hz. Such voltage variations require dynamic compensation by for example a static var compensator (Kundur, 1994) and are out of scope for the emergency control studied in this test case. The reactive demand from loads close to generation areas is often supplied by the generators and by the less expensive static devices, such as shunt capacitor banks and reactors, in load areas far from generators. It is however not unusual to install capacitor banks in combination with dynamic devices to increase the effective control range of these devices.

Steady-state Characteristics of Compensation Devices

Referring to the *pv*-curves shown in Figure 12, the effect of the control measures will be discussed in terms of their effect on the system stiffness, critical voltage and the theoretical and practical transfer limits. Increased stiffness is beneficial for the robustness of the system since it implies a smaller voltage change for a certain change in the load. Increasing the critical voltage is generally detrimental to system robustness since it increases the voltage at which voltage instability occurs[2]. The separation of the theoretical and practical transfer limits can be used as a measure of the system robustness against load change.

The shape of the *pv*-curve of the uncompensated system depends on the power factor of the load as well as the impedance of the line and the feeding end voltage. The load is now supplied through an ideal tap changing transformer and shunt compensation is connected at the load bus, below the transformer, where applicable. Series compensation is inserted in series with the line impedance. The base case with no compensation corresponds to the system in Figure 9 with $E = 1, X = 1$ and $\tan(\phi) = 0$.

Shunt capacitors act by adding capacitive admittance to the load and can thereby adjust the power factor of the load as seen from the transmission system. The amount of reactive power generated by a capacitor is quadratically dependent on the voltage so it will provide less support at low voltages. Compensation by capacitor banks increases the practical transfer limit but also increases the critical voltage and decreases the stiffness of the system. The theoretical and practical transfer limits are brought closer together. The injection of a fixed amount of reactive power at the load bus, for example by a generator, increases the critical voltage less than the corresponding amount of shunt capacitor and is less detrimental to the stiffness of the system. In addition, the injection of a fixed amount of reactive power increases the theoretical and practical transfer limits more than the corresponding amount of capacitor compensation. Shunt reactors have the opposite effect compared to capacitor banks and are sometimes used to absorb excess reactive power produced by lightly loaded lines and cables.

[2]Assuming constant power load characteristics (Pal, 1992)–the system may still be stable for other load characteristics.

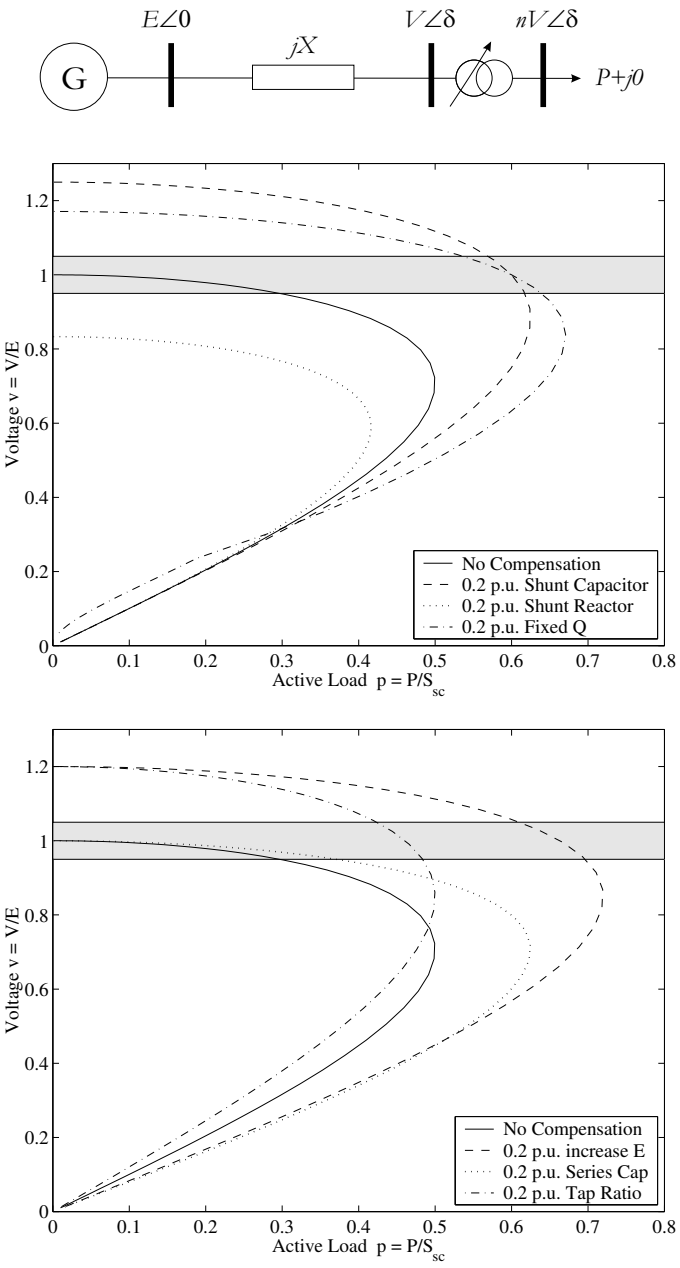

Figure 12: The effect of various compensation devices in the *pv*-plane.

Generators normally operate in voltage control mode in which an *automatic voltage regulator* (AVR) acts on the exciter of a synchronous machine. The exciter supplies the field voltage and consequently the current in the field winding. Within the capability limits of the machine, it can thereby regulate the voltage of the bus where it is connected. The response time of the primary controllers is short, typically fractions of a second, for generators with modern excitation systems. The amount of reactive power that a generator must produce to regulate the voltage depends on the structure and load situation of the surrounding transmission system.

Series capacitances are connected in series with the line inductance and can lower the apparent reactance of a line and thereby scale the pv-curve along the p-axis. This increases the maximum transfer capability of the line without increasing the critical voltage and thereby keeps the theoretical and practical transfer limits separated. The stiffness of the system is improved and series capacitors would appear to be the ideal compensation device. They have however, a reputation of causing subsynchronous resonance and need complicated protection equipment to protect them from fault currents (Kundur, 1994). They are therefore not in widespread use for the purpose of alleviating voltage problems, since voltage problems are often less expensively solved using shunt compensation. Although the installation of series capacitors most often has been motivated by other types of stability problems, they do however contribute to improved voltage control where they have been installed.

Power transformers with on-load tap changers can scale the pv-curve along the v-axis and thereby increase the practical but not the theoretical transfer limit. Transformers equipped with tap changers can shift reactive power between their primary and secondary sides and thereby regulate the voltage of their low voltage side. The regulation of the low side voltage however affects the voltage at the high voltage side in the opposite direction. This effect is small under normal operation but may be a significant factor in voltage instability incidents such as described in Section 5.6. When the tap ratio is increased, stiffness of the system is sacrificed and the practical transfer limit moves closer to the theoretical limit.

An increase of the feeding voltage E scales the pv-curve along both axes and thereby increases the practical and theoretical transfer limits. The stiffness is slightly decreased and the practical and theoretical transfer limits are brought closer together. Note however that the control range of the feeding voltage is usually limited since both line ends must comply with the practical voltage limit.

Similarly to the production of reactive power by shunt capacitor banks, the generation by cables and overhead lines is quadratically dependent on the voltage and has a similar detrimental effect on the system stiffness.

5.3 Tap Changer Control Systems

An early detailed description of a typical tap changer control system was given in Ćalović (1984). The proposed tap changer model was a complex nonlinear

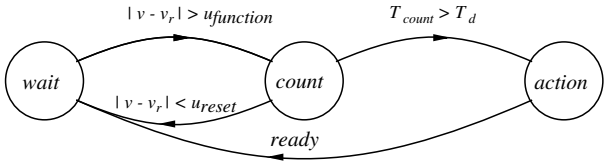

Figure 13: State graph illustrating function of a non-sequential OLTC control system.

dynamic model that encompassed some inherent time delays. More recent work presented in Sauer and Pai (1994) explored further the tap changer modelling issue, and presented simpler yet still accurate models. Depending on the OLTC characteristic (type of time delay), various discrete state dynamic models and corresponding continuous approximations were derived.

The state graph in Figure 13 illustrates the function of a typical OLTC control system. The system remains in the state **wait** as long as the voltage deviation ($|v - v_r|$) is less than the function voltage (v_{function}). When the limit is exceeded, a transition to the state **count** occurs. Upon entering **count**, a timer is started and is kept running until either it reaches the delay time T_d, causing a transition to the state **action**; or the voltage deviation becomes less than the reset voltage (v_{reset}), causing a transition to the state **wait** and reset of the timer. When entering the state **action**, a control pulse to operate the tap changer is given. After the mechanical delay time (T_m), the tap operation is completed and the control system receives a **ready** signal from the tap changer. The control system then returns to state **wait**.

The time delay is tuned by the time delay parameter T_{d0}. The actual time delay can then be either fixed ($T_d = T_{d0}$), or inversely proportional to the voltage deviation ($T_d \sim T_{d0}/|v - v_r|$), depending on the control system.

Two types of time domain charact-eristics are used in conventional tap changer control systems. The simplest is the constant time variant, where the time delay T_d is constant. With inverse-time character-istics the time delay is dynamically updated according to some formula, for example inversely proportional to the voltage deviation.

5.4 Voltage Sensitivity of Loads

So far, we have assumed that the apparent admittance of the load is constant. However, the admittance of many loads varies with the supply voltage–either by their inherent design or by control loops connected to the load devices. Typical examples of such loads are motor drives equipped with power-electronic converters and thermostatically controlled heating devices, which adjust their apparent admittance in order to consume constant power. The composite load seen from the transmission level often contains a significant amount of induction motor loads, which exhibit potentially very complex voltage behaviour. However, for

small voltage excursions, say less than 10 %, the active power drawn by induction motors can in the long term be approximated as constant and the reactive power as proportional to an exponential of the voltage. The dynamic response of loads to voltage changes plays a major role in the analysis and evolution of voltage instability. Simplifying matters somewhat, the load as seen from the transmission level can normally be considered as constant power in the long term since it is connected through tap changers that keep the load voltages close to their nominal values.

There are two fundamentally different approaches to the modelling of voltage dependency of the aggregate load at a high-voltage bus. One method is to start from models of the individual load devices and aggregate them according to the load composition below a certain point in the network. The main advantage of this approach is that the load parameters have a physical meaning. Since each load device is physically modelled, it is reasonable to assume that these aggregated models are appropriate for large disturbances, provided that the individual component models and their parameter values are appropriate. Drawbacks of this method are the difficulty of knowing the true load composition and the large computational complexity when these models are used for simulation. A survey on this type of load modelling is given in IEEE (1995).

The other approach, referred to as generic load modelling, employs parameter estimation methods and black-box modelling. Parameter values in a nominal model structure can be mathematically extracted from a recorded load response to a known disturbance. A disadvantage with these models is that they can usually only be trusted to be reliable under the same loading conditions and for the same type of disturbance as were applied when the recordings were done. Control design on the basis of this type of model would require on-line parameter estimation or a conservative choice of parameter values based on extensive field measurements. The load model used throughout this thesis was proposed by Karlsson (1992) through the parameter estimation approach to load modelling. Load parameter values obtained over a wide range of operating conditions were also given. The model is based on the assumption that most load devices have an instantaneous voltage dependency resulting in an instantaneous load relief if the supply voltage decreases, and a steady-state voltage dependency that gives a lasting load relief. The instantaneous dependency is generally stronger than the steady-state dependency. The load model structure is:

$$T_p \frac{\mathrm{d}x_p}{\mathrm{d}t} = -x_p + P_s(V) - P_t(V) \tag{13}$$

$$P_d = x_p + P_t(V) \tag{14}$$

where x_p is an internal state modelling the load recovery dynamics. The active power load model is parameterized by the steady-state voltage dependency $P_s(V) = P_0 V^{\alpha_s}$, the transient (instantaneous) voltage dependency $P_t(V) = P_0 V^{\alpha_t}$ and a recovery time constant T_p. P_d is the actual active power load and P_0 is the sum of the rated power of the loads connected. A similar model is used for the reactive power, with corresponding characteristics $Q_s(V) = Q_0 V^{\beta_s}$,

T_p	T_q	α_s	α_t	β_s	β_t
60-300 s	30-200 s	0-2	1-3	2-5	4-6

Table 1: Typical parameter values for the load model given by Equations (13)-(14). Adapted from Karlsson and Hill (1994).

$Q_t(V) = Q_0 V^{\beta_t}$ and recovery time constant T_q. The voltage V is here normalized using the nominal voltage of the bus where the load is modelled. Typical parameter values are shown in Table 1.

When the load dynamics are fully recovered and the load is supplied at nominal voltage, the actual load demand is equal to the sum of the ratings of all connected load devices. This model is a special case of the generalized framework for black-box load models presented in Karlsson and Hill (1994). A generic model that includes also the effects of varying voltage phase angle has been presented by Ju et al. (1996). Results from field measurements on the BC Hydro system were presented by Xu et al. (1997), based on a generic load model structure presented in Xu and Mansour (1994). More recent work has used higher-order load models to account for the effect of cascaded tap changers in the downstream load (Lind and Karlsson, 1996; le Dous, 1999).

The response of a power system model to critical disturbances is highly dependent on the load representation used. Borghetti et al. (1997) make a comparison between the responses of detailed induction motor load models and a generic exponential recovery load model, and conclude that a detailed representation of induction motors is required in voltage stability studies of systems with a significant amount of induction motor load. Arnborg et al. (1998) compare the system response with different types of generic dynamic load models and conclude that the type of load representation used can affect the qualitative behaviour of the system, even if the load models exhibit the same response to a nominal disturbance, such as the one applied when the load recordings were done. Despite this potential drawback of the generic load models, they are often the best choice available since the values of their parameters can be extracted from off-line experiments or even by on-line estimation. The discrepancies found when comparing generic load models and detailed induction motor models present themselves mainly at very low voltages, say at less than 90 % of rated voltage. If the voltage is kept higher than that by appropriate emergency control, the generic load models can be expected to be accurate as long as the choice of parameter values is appropriate. An early approach to on-line estimation of load parameter values was presented by Dovan et al. (1987).

5.5 Voltage Stability

The *voltage stability* of power systems basically implies its capability of reaching and sustaining an operating point in a controllable way following a disturbance, and that the steady-state post-disturbance system voltages are acceptable. More

formal definitions can be found for example in Van Cutsem and Vournas (1998). Furthermore, the term *voltage instability* denotes the absence of voltage stability and *voltage collapse* the transition phase during which a power system progresses towards an unacceptable operating point due to voltage problems, often resulting in blackouts or separation of the system into separate unsynchronized islands.

The dynamics of voltage phenomena can be divided into the two main groups: short- and long-term dynamics. Short-term phenomena act on a time scale of seconds or shorter and include, for example, the effect of generator excitation controls, induction motor recovery/stalling dynamics and FACTS[3] devices. The long-term dynamic phenomena act on a time scale of minutes and include, for example, the effect of recovery dynamics in heating load and the effect of generator overcurrent protection systems. A detailed categorization of phenomena into the short- and long-term categories is given in Van Cutsem and Vournas (1998).

As discussed in the previous section, many loads respond to a voltage drop by increasing their apparent admittance. Assume that the load supplied by the network in Figure 9 has such a recovery mechanism according to the normalized model

$$T\,\frac{\mathrm{d}g}{\mathrm{d}t} = p_0 - p \tag{15}$$

$$p = g\,v^2 \tag{16}$$

Thus, the load has instantaneous admittance characteristics but also an internal controller that aims to restore the power drawn to constant power p_0 with the time constant T s. Furthermore, assuming that the load is purely active ($\tan(\phi)$=0) and combining (12) and (15)-(16), the full model can be written in the differential-algebraic form

$$T\,\frac{\mathrm{d}g}{\mathrm{d}t} = p_0 - gv^2 \tag{17}$$

$$v = \frac{1}{\sqrt{g^2+1}} \tag{18}$$

Substituting (18) in (17) yields

$$f(g) = \frac{\mathrm{d}g}{\mathrm{d}t} = \frac{1}{T}\left(p_0 - \frac{g}{1+g^2}\right) \tag{19}$$

Solving for stationary points yields the two solutions

$$g^* = \frac{1}{2p_0} \pm \sqrt{\frac{1}{4p_0^2} - 1} \tag{20}$$

Thus, we can conclude that there are two separate equilibria if $p_0 < 0.5$ that coalesce for $p_0 = 0.5$. For $p_0 > 0.5$ there appears to be two separate equilibrium

[3]Flexible AC Transmission System

points with complex g. But g is real-valued since we have defined it as the real part of the admittance phasor in equation (9). Thus, we can conclude that there are no equilibria for $p_0 > 0.5$ and that a *loss of equilibrium* occurs when p_0 increases beyond 0.5. Since (19) is always positive for $p_0 > 0.5$, the admittance will increase towards infinity (or an internal limit in the load device) and the load voltage will approach zero. Small-disturbance stability analysis (Kahlil, 1992) can be used to determine that for $p_0 < 0.5$, the low admittance solution corresponding to the upper half of the *pv*-curve is asymptotically stable and the high admittance solution on the lower half is unstable.

Figure 14 shows simulation results with the initial state at the stable and unstable equilibria for $p_0 = 0.3448$, respectively. At simulation time 20 s, the load setpoint is increased to $p_0 = 0.4$. From (20) we see that for the given initial value of the active power load, there are two possible solutions:

- The load operates in the stable equilibrium (a) on the upper part of the *pv*-curve. When the load setpoint is increased, the load increases its admittance and the operating point moves toward (a') to the right on the *pv*-curve. This corresponds to higher active power transfer on the line and the load settles at the new equilibrium point (a') with a slightly lower voltage and the load consumption at its new setpoint. The combined load and transmission system is thus stable.

- The load operates in point (b) on the lower part of the *pv*-curve. When the load setpoint is increased, the load increases its admittance and the operating point moves to the left on the *pv*-curve. This corresponds to even lower load consumption and the load increases its admittance further, moving the operating point further to the left and so on. Thus, the operating point is unstable and the system will approach the point (0,0) in the *pv*-plane.

Assuming constant power load characteristics as above, the theoretical transfer limit marked by the dashed curve in Figures 10–11 therefore also becomes a steady-state voltage stability limit. However, note that the operating point may transiently move to the unstable lower part and back again to the stable equilibrium on the upper part of the *pv*-curve. Analogously, there is no guarantee that the system will reach a stable operating point simply because such an operating point exists. A trajectory will only approach the stable equilibrium as long at it remains within the *region of attraction* of the stable equilibrium. Such regions of attraction can be approximately computed using a Lyapunov-method for general dynamical systems, but the problems of finding a good Lyapunov-function may make the results conservative (Kahlil, 1992). Vu and Liu (1992) present other analytical methods for computation of such stability regions. In the simple case studied here, the region of attraction can be found exactly, and is bounded by point (b) on the *pv*-curve in Figure 14. That is, for all initial conditions with an admittance value smaller than that corresponding to the unstable equilibrium, the system will approach the stable equilibrium. Since the equilibrium point (b) is unstable, it has no region of attraction. Operating

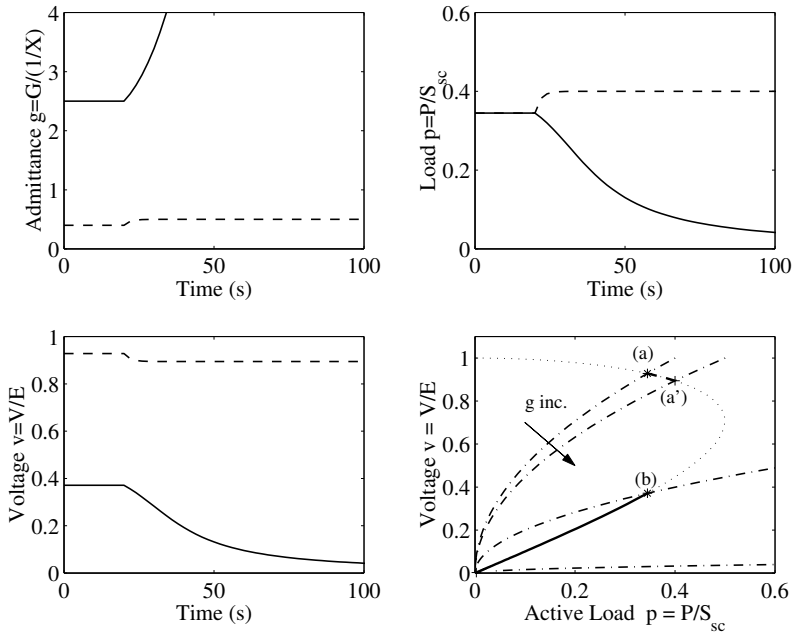

Figure 14: Illustration of voltage instability due to load recovery dynamics. Dashed curves correspond to the stable case, and the solid curves to the unstable case. The dotted line is the pv-curve and the dash-dotted lines correspond to (transient) load characteristics for different g.

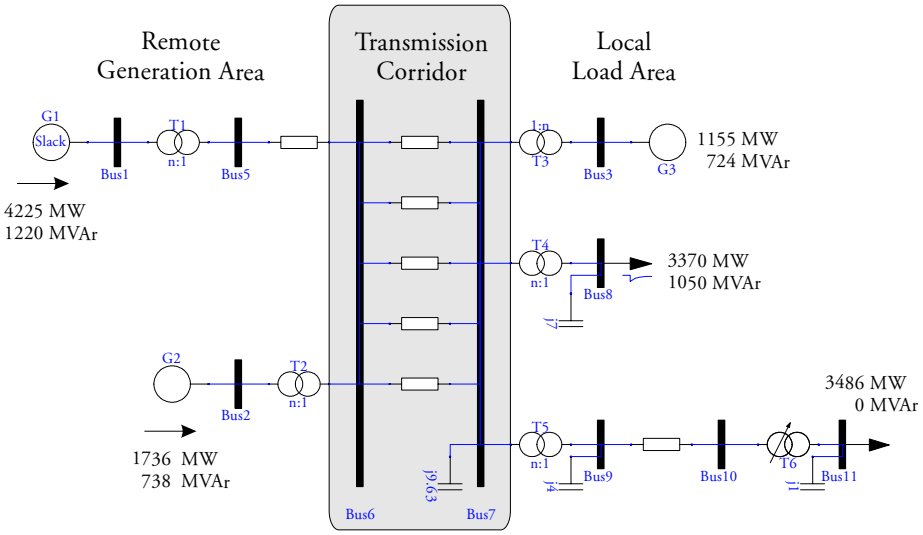

Figure 15: The BPA test system (CIGRE, 1995).

points on the lower half of a *pv*-curve can still be stable with other load characteristics than constant power. For example, all operating points are stable when the steady-state load characteristic is constant impedance.

5.6 Case Study - BPA Test System

Figure 15 shows a one-line diagram of the BPA[4] test system (CIGRE, 1995) that will be used to illustrate some of the mechanisms of voltage instability by time simulation. The system has most of its generation in a remote area that is connected to a main load area through five transmission lines. Most of the load is supplied by generators G1 and G2 in the remote generation area and is transported to the load area through the transmission lines. Generator G3 in the local area supplies a small amount of active power, but another important role is to regulate the voltage at Bus 7, to maximize the transfer capability of the lines of the transmission corridor.

Generator G1 is modelled as an infinite bus and generators G2 and G3 using 6th-order dq-models with IEEE ST1A excitation systems and integral-type overexcitation limiters. The load at bus 8 is modelled with instantaneous constant impedance characteristics but recovers to constant power load with a time constant of 1 s. The load at bus 11 is modelled as a constant impedance and is connected through the tap changing transformer T6. The transformer T6 is controlled by an inverse-time relay according to model *D3* in Sauer and Pai (1994) that adds load recovery dynamics to the load at bus 11. The full simulation model in ObjectStab format can be downloaded from Larsson

[4]Bonneville Power Administration (`http://www.bpa.gov`)

(2000b).

Figure 16 shows simulation results of a fault and the subsequent disconnection of one of the five parallel lines at simulation time 10 s. The course of events is fairly typical for voltage instability incidents triggered by a fault in the transmission system.

1. At time 10.07 s, the fault is cleared and the line is disconnected.

2. At approximately time 13 s, the short-term dynamics which include the generator electromechanical and the fast load recovery dynamics at bus 8 have settled. The voltages at buses 8 and 11 settle at 0.89 and 0.9 p.u., respectively, and the field currents of both G2 and G3 are below their overexcitation limits. Since the voltage at bus 11 is below the OLTC deadband, its internal timer is started.

3. At time 22.5 s, the OLTC makes its first operation and slightly increases the voltage of bus 11, however it is still below the tap changer deadband. The OLTC operation further depresses the voltage of Bus 10 and increases the reactive power demand from generator G3, which now exceeds its overexcitation limit and its internal timer is started.

4. At time 32.5 s, the overexcitation limiter limits the field voltage of the generator G3 to its internal setting at 2.9 p.u., and voltage support of the load area end of the transmission corridor is lost.

5. Between times 37-97 s, the tap changer of T6 operates and aims to restore the voltage of bus 11. However, the tap changer also increases the apparent admittance of the load at bus 11 and thereby puts additional strain on the transmission system. Since G3 is now unable to supply the necessary reactive power to regulate the voltage at bus 7, the voltage decreases further and consequently the reactive losses in the lines of the transmission corridor increase. The increased reactive power demand must now be supplied from the remote generators G1 and G2, and G2 reaches its limit at approximately time 87 s. The limiter is activated ten seconds later.

6. After time 97 s, with both generators G2 and G3 at their field limitations, the voltages of both bus 6 and bus 7 decrease and the transfer capability of the lines in the transmission corridor is further decreased. The tap changer of T6 makes two more operations and is now at its maximum setting. Hereafter, the load recovery dynamics of the load at bus 8 drive the final stage of the collapse until the simulation terminates at time 160 s.

We observe, in agreement with for example Taylor (1994) and Kundur (1994) who have made similar studies of the BPA test system, that the voltage collapse is due to a complex interaction of the following factors:

- The apparent impedance and consequently the voltage drop and losses across the lines of the transmission corridor increase when the line has been disconnected.

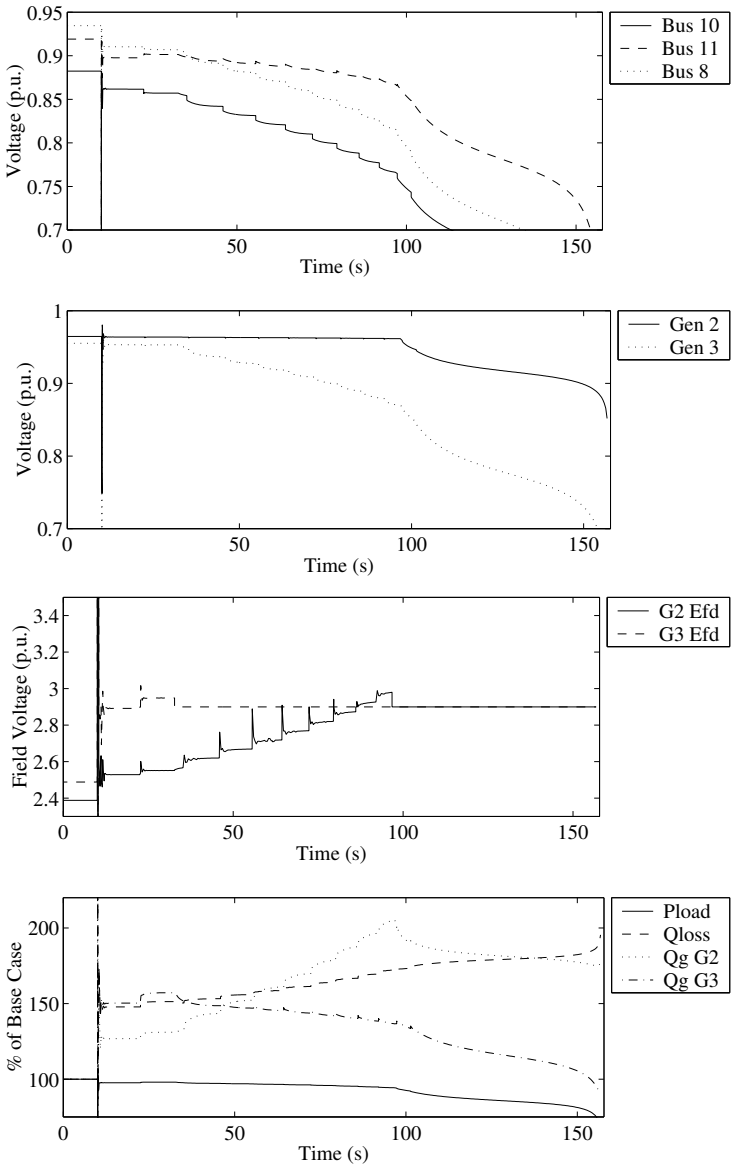

Figure 16: Simulation results illustrating voltage collapse in the BPA test system. Pload denotes the sum of the active load as buses 8 and 11, and Qloss denotes the reactive losses in the lines of the transmission corridor.

- The load recovery dynamics of the load at bus 8 and the combined transformer and constant impedance load at bus 11 are unfavourable, since they aim to restore the load demand even at the reduced voltage.
- After the overexcitation limiters have been activated, the generators are unable to supply enough reactive power to compensate for the increased losses in the lines of the transmission corridor, and consequently they can no longer regulate their respective terminal voltages.

Other mechanisms that can cause or play a significant role in voltage collapse phenomena include; line protection, the response of governor and automatic generation controls following generation outage, the control limits of FACTS devices and rapid load increase (Kundur, 1994). As illustrated above, voltage collapses are often cascades of events, with many contributing factors, that leads to the final breakup of the system. Arnborg (1997, and references therein) describe the course of events in several actual voltage collapses.

5.7 Countermeasures Against Voltage Collapse

Many countermeasures against voltage collapse have been proposed (CIGRE, 2000). Some examples are undervoltage load shedding, switching of capacitor banks, activation of fast-starting generation, rescheduling of active and reactive power generation, and locking or backstepping of tap changers. The effect of some of these countermeasures can be understood from the pv-curves shown in Figure 17.

Assume again that the combined network and load is modelled by the model (17)–(18). Thus, the purely active load has instantaneous constant impedance characteristics but recovers to constant power with a time constant. Referring to the left figure in Figure 17, assume that the load has the internal setpoint set at $p_0 = 0.55$, that is, its steady-state load characteristic is given by the line (a). There is then no intersection of the steady-state load characteristic and the pv-curve. Such a situation can present itself following a rapid load increase or, perhaps more likely, due to the tripping of transmission lines. Based on the observations on pages 21–24, we can conclude that voltage collapse will occur due to loss of equilibrium. Load shedding can be modelled by decreasing the load setpoint p_0. The load characteristic (a') corresponds to $p_0 = 0.45$ and has two intersections with the pv-curve, each corresponding to an equilibrium point. Again, based on the observations on pages 21–24, we can conclude that one of those is stable. Thus, load shedding appears to be a way of stabilizing the system in case of voltage instability.

Figure 18 illustrates the effect of load shedding in the BPA test system using undervoltage load shedding relays as proposed by Vu et al. (1995). At time 93.5 s, the voltage at bus 8 decreases below the load shedding threshold at 0.82 p.u., and 1.5 s later the relay sheds 5 % of the load at bus 8. The OLTC of transformer T6 then makes two more operations to restore the voltage at bus 11 and all voltages settle to stable values. The load reduction corresponds to about 3 % of the combined pre-disturbance load at buses 8 and 11.

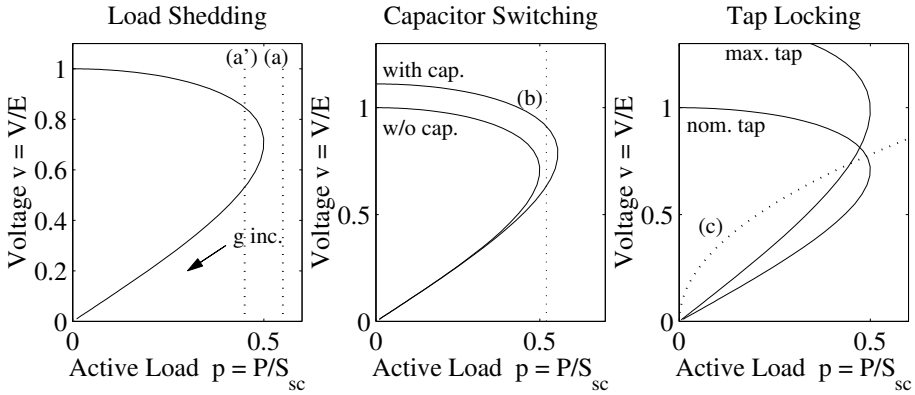

Figure 17: Illustration of various countermeasures against voltage collapse. The solid lines are pv-curves with constant $tan(\phi)$ and the dotted lines correspond to steady-state load characteristics.

Referring to the middle figure in Figure 17, the connection of a capacitor bank at the load end can improve the apparent power factor of the load and create equilibrium points on a new, more favourable, pv-curve. Assume again that the load has steady-state constant power characteristics given by the line (b). Then there are no equilibrium points without a capacitor bank, and voltage collapse will occur due to loss of equilibrium. Switching in a capacitor bank will create two new equilibrium points given by the intersections of the new pv-curve and the steady-state load characteristics. It can be concluded in the same way as for load shedding that one of these equilibrium points is stable.

Referring to the right figure in Figure 17, as tap changers increase their ratio, the pv-curve is scaled along the v-axis. Suppose now that the load has constant impedance steady-state characteristics as indicated by the figure. The load thus lacks the recovery dynamics assumed earlier in this section. Based on results presented for example by Pal (1995), we can thus conclude that any intersection of the (constant impedance) steady-state load characteristic and the pv-curve would indicate the existence of a stable equilibrium point. Suppose that the operating point is in the stable equilibrium given by the intersection of the nominal tap pv-curve and the load characteristic. If the voltage here is lower than the voltage defined by the control system deadband, the tap ratio will increase towards the maximum tap unless the tap is locked. Under normal operation this would correspond to increased load side voltage–standard relay controllers for tap changers make that assumption–but due to the high load in the case considered, the voltage actually decreases further as the tap ratio is increased. By locking the tap changer, the destabilizing control loop is broken and the controlled voltage can settle at a low but stable voltage. The sign change in the effect of tap changer control is known as the reverse action phenomena and is described in for example Ohtsuki et al. (1991). The effect of tap changer

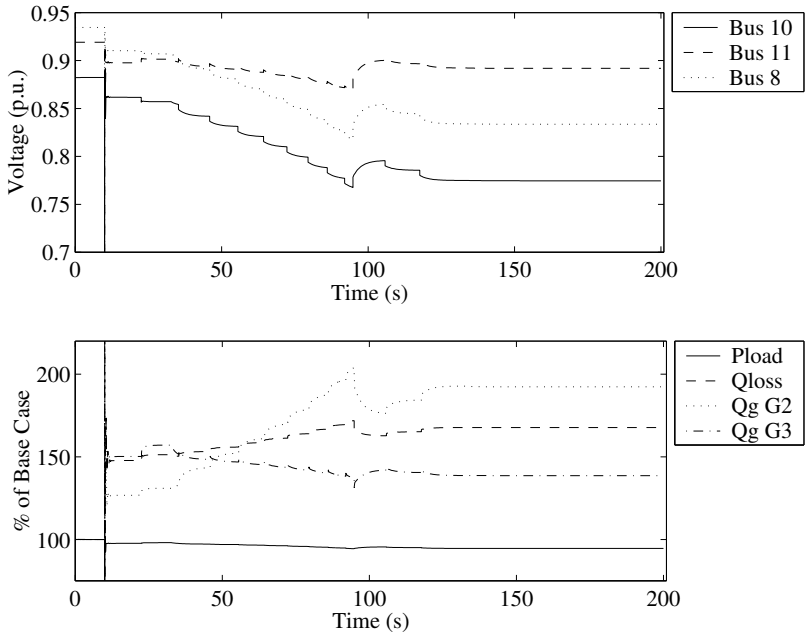

Figure 18: Simulation results illustrating successful stabilization of the voltages in the BPA test system by undervoltage load shedding of 5 % of the load at bus 8 at simulation time 95 s.

controls is a major factor in the development of voltage collapse, especially where there are cascaded tap changers and when their effect is combined with the effect of generator current limiters. The effect of tap locking is highly dependent on the steady-state load characteristics. For tap locking to be an effective control, the load must have a high degree of steady-state voltage dependence. If the load has instantaneous constant power characteristics and is connected directly to the transformer, tap locking has no effect at all (Pal, 1995).

Figure 19 illustrates the effect of tap locking in the BPA test system. At time 82.5 s, the voltage at the primary side of transformer T6 decreases below the tap locking threshold at 0.82 p.u. and the tap is immediately locked. The voltages then settle at stable values. Since the voltage at bus 11 is lower than the pre-disturbance voltage, it draws less power than at the pre-disturbance operating point. Although the voltage at Bus 11 may be unacceptably low, the collapse has been arrested and the time frame within which other emergency controls can be taken has been extended. The load reduction corresponds to about 5 % of the combined pre-disturbance load at buses 8 and 11.

Note that the discussion above considers only the *existence* of stable operating points and consequently whether or not it is at all possible to stabilize the system using the considered countermeasures. Also, quite strong assumptions on the steady-state load characteristics are made, such as that they are constant

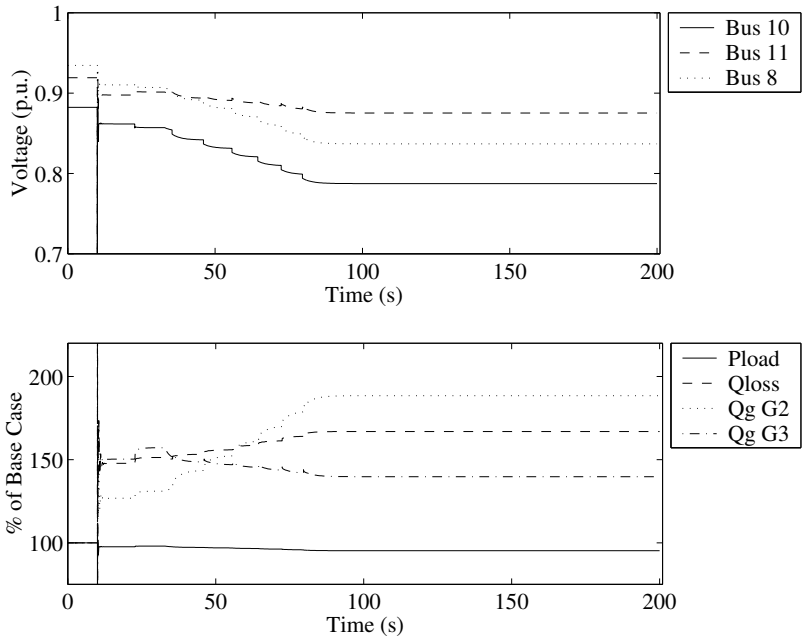

Figure 19: Simulation results illustrating successful stabilization of the voltages in the BPA test system by locking of the tap changer of T6 at simulation time 81 s.

power and constant impedance. To guarantee attraction to the stable equilibria created by the countermeasures, also transient load characteristics and the issues of regions of attraction must be considered. In turn, this implies that proper timing of emergency control is also necessary. The discussion of these issues is however out of scope of this introductory chapter. Detailed studies of load shedding, accounting for transient load characteristics in aggregate load models are given for example in Xu and Mansour (1994); Arnborg et al. (1998); Pal (1995); Balanathan et al. (1998). Similar studies on capacitor switching are given in for example Vu and Liu (1992); Pal (1995) and on tap locking in Vu and Liu (1992); Popović et al. (1996). A general conclusion that can be made regarding the use of these countermeasures is that exact and well-timed control actions are necessary, and that their effect is highly dependent on the current operating point and the load characteristics.

The current limiters of generators G2 and G3 played a central role in the voltage collapse in the BPA test system studied in the previous section. Starting emergency generation at the load end will support the load end with reactive as well as active power, reduce the load of the limited generators and support the voltage at the load end. Even if the limited generators are not taken out of their limits, the support may be enough to arrest a voltage collapse. When generators situated at the load end that are equipped with armature current limiters reaches

their armature limit, it may be beneficial to reduce their active power production and thereby increase their capacity of supplying reactive power (Johansson, 1999). Another approach is to include "soft" generator current constraints, allowing temporary overloading of a generator to utilize the thermal capacity of the generator windings (Johansson and Daalder, 1997). Soft current constraints may not be enough to arrest a collapse by themselves, but may slow the speed of the collapse and thereby provide time to take other emergency control actions.

References

Arnborg, S. (1997). *Emergency Control of Power Systems in Voltage Unstable Conditions*. Ph.D. thesis, Royal Institute of Technology, Sweden.

Arnborg, S., Andersson, G., Hill, D. J. and Hiskens, I. A. (1998). On influence of load modelling for undervoltage load shedding studies. *IEEE Transactions on Power Systems*, vol. 13, no. 2, pp. 395–400.

Balanathan, R., Pahalawaththa, N. C., Annakkage, U. D. and Sharp, P. W. (1998). Undervoltage load shedding to avoid voltage instability. *IEE Proceedings Generation, Transmission and Distribution*, vol. 145, no. 2, pp. 175–81.

Borghetti, A., Caldon, R., Mari, A. and Nucci, C. A. (1997). On dynamic load models for voltage stability studies. *IEEE Transactions on Power Systems*, vol. 12, no. 1, pp. 293–303.

Ćalović, M. S. (1984). Modelling and analysis of under-load tap-changing transformer control system. *IEEE Transactions on Power Apparatus and Systems*, vol. PAS-103, no. 7, pp. 1909–15.

CIGRE (1995). *Long Term Dynamics Phase II*. Tech. rep., CIGRE Task Force 38.02.08.

CIGRE (2000). *System Protection Schemes in Power Networks*. Tech. rep., CIGRE Task Force 38.02.19.

Dovan, T., Dillon, T. S., Berger, C. S. and Forward, K. E. (1987). A microcomputer based on-line identification approach to power system dynamic load modelling. *IEEE Transactions on Power Systems*, vol. PWRS-2, no. 3, pp. 529–536.

Elmqvist, H., Brück, D. and Otter, M. (2000). *Dymola, Users Manual*. Dynasim AB, Sweden. `http://www.dynasim.se`.

IEEE (1995). Standard load models for power flow and dynamic performance simulation. *IEEE Transactions on Power Systems*, vol. 10, no. 3, pp. 1302–1313.

Johansson, S. G. (1999). Mitigation of voltage collapse caused by armature current protection. *IEEE Transactions on Power Systems*, vol. 14, no. 2, pp. 591 – 9.

Johansson, S. G. and Daalder, J. E. (1997). Maximum thermal utilization of generator rotors to avoid voltage collapse. In *IPEC '97. Proceedings of the International Power Engineering Conference.*, vol. 1, pp. 234–9. Nanyang Technol. Univ, Singapore.

Ju, P., Handschin, E. and Karlsson, D. (1996). Nonlinear dynamic load modelling: model and parameter estimation. *IEEE Transactions on Power Systems*, vol. 11, no. 4, pp. 1689–1697.

Kahlil, H. K. (1992). *Nonlinear Systems*. Macmillan Publishing Company. ISBN 0-02-946336-X.

Karlsson, D. (1992). *Voltage Stability Simulations using Detailed Models Based on Field Measurements*. Ph.D. thesis, Electrical and Computer Engineering, Chalmers Institute of Technology, Sweden.

Karlsson, D. and Hill, D. J. (1994). Modelling and identification of nonlinear dynamic loads in power systems. *IEEE Transactions on Power Systems*, vol. 9, no. 1, pp. 157–63.

Kundur, P. (1994). *Power System Stability and Control*. Power System Engineering Series. McGraw-Hill, New York. ISBN 0-07-035958-X.

Larsson, M. (2000a). *Coordinated Voltage Control in Electric Power Systems*. Ph.D. thesis, Industrial Electical Engineering and Automation, Lund University, Sweden. `http://www.iea.lth.se/~ielmatsl/Publications/thesis.html`.

Larsson, M. (2000b). Thesis website. `http://www.iea.lth.se/~ielmatsl/Publications/thesis.html`.

Larsson, M., Popović, D. H. and Hill, D. J. (1998). Limit cycles in power systems due to OLTC deadbands and load-voltage dynamics. *Electric Power Systems Research*, vol. 47, no. 32, pp. 181–8.

le Dous, G. (1999). *Voltage Stability in Power Systems - Load Modelling based on 130 kV Field Measurements*. Tech. Rep. 324L, Chalmers University of Technology, Sweden. Licentiate Thesis.

Lind, R. and Karlsson, D. (1996). Distribution system modelling for voltage stability studies. *IEEE Transactions on Power Systems*, vol. 11, no. 4, pp. 1677–82.

Ohtsuki, H., Yokoyama, A. and Sekine, Y. (1991). Reverse action of on-load tap changer in association with voltage collapse. *IEEE Transactions on Power Systems*, vol. 6, no. 2, pp. 300–6.

Pal, M. K. (1992). Voltage stability conditions considering load characteristics. *IEEE Transactions on Power Systems*, vol. 7, no. 1, pp. 243–9.

Pal, M. K. (1995). Assessment of corrective measures for voltage stability considering load dynamics. *International Journal of Electrical Power & Energy Systems*, vol. 17, no. 5, pp. 325–34.

Popović, D. H., Hill, D. J. and Hiskens, I. A. (1996). Oscillatory behaviour of power supply systems with single dynamic load. In *Proceedings 12th Power Systems Computation Conference, Dresden, Germany*.

Sauer, P. W. and Pai, M. A. (1994). A comparison of discrete vs. continuous dynamic models of tap-changing-under-load transformers. In *Proceedings Bulk Power System Voltage Phenomena - III : Voltage Stability, Security and Control, Davos, Switzerland*.

Taylor, C. W. (1994). *Power System Voltage Stability*. McGraw-Hill. ISBN 0-07-063184-0.

Taylor, C. W. (2000). Minutes of preliminary meeting of Cigre TF 38.02.23 on coordinated voltage control in transmission networks, Seattle, USA.

Tiller, M. (2001). *Introduction to Physical Modelling with Modelica*. No. ISBN 0792373677. Kluwer Academic Publishers.

Van Cutsem, T. and Vournas, C. (1998). *Voltage Stability of Electric Power Systems*. Power Electronics and Power Systems Series. Kluwer Academic Publishers. ISBN 0-7923-8139-4.

Vu, K. T. and Liu, C.-C. (1992). Shrinking stability regions and voltage collapse in power systems. *IEEE Transactions on Circuits & Systems I-Fundamental Theory & Applications*, vol. 39, no. 4, pp. 271–89.

Vu, K. T., Liu, C.-C., Taylor, C. W. and Jimma, K. M. (1995). Voltage instability: mechanisms and control strategies. *Proceedings of the IEEE*, vol. 83, no. 11, pp. 1442–55.

Xu, W. and Mansour, Y. (1994). Voltage stability analysis using generic dynamic load models. *IEEE Transactions on Power Systems*, vol. 9, no. 1, pp. 479–93.

Xu, W., Vaahedi, E., Mansour, Y. and Tamby, J. (1997). Voltage stability load parameter determination from field tests on B.C. Hydro's system. *IEEE Transactions on Power Systems*, vol. 12, no. 3, pp. 1290–7.

Yorino, N., Danyoshi, M. and Kitagawa, M. (1997). Interaction among multiple controls in tap change under load transformers. *IEEE Transactions on Power Systems*, vol. 12, no. 1, pp. 430–6.